To be published in the SPACEOPS 2023 Conference Proceedings, The 17th International Conference on Space Operations, 6 – 10 March 2023, Dubai, United Arab Emirates

GNSS-Multicarrier-Broadband-Waveform Satellite System Emulator

Josselyn Romero[1], Leonardo Amador[2], Tien M. Nguyen[3], Charles H. Lee, Yinwei Chen[4], and Sam Behseta
California State University
Fullerton, California, USA

Dan Shen, Genshe Chen, John Nguyen and Xiwen Kang
Intelligent Fusion Technology
Germantown, Maryland
USA

Khanh D. Pham
Air Force Research Laboratory
Space Vehicles Directorate
Kirtland AFB
New Mexico, USA

Abstract

This paper describes a satellite system emulator that can emulate a newly proposed Global Navigation Satellite System-Multi-Carrier Broadband Waveforms (GNSS-MCBBW) in the presence of non-ideal system components and imperfect operational conditions. The non-ideal system components include RF up-converter, balanced modulator, phase modulator, RF filter, and high-power amplifier (HPA). The imperfect operational conditions consist of the system operating temperature and input back-off power (IPBO) of the HPA. The emulator can emulate GNSS-MCBBW signals using Hilbert Transform (HT) and bandpass filter (BPF) signal processing techniques. In addition, the emulator can also emulate an ideal pre-distorter (PD) that can be used for the evaluation of HPA PD using machine learning and artificial intelligence (ML-AI). The objective of this paper is to describe the MATLAB implementation approach for the non-ideal GNSS-MCBBW system component models in the presence of imperfect system temperature and HPA IPBO operational conditions and provide simulation results to demonstrate the utility of the emulator.

1. Background and Introduction

Our research team, consisting of IFT and CSUF teams, addresses the SBIR Phase 2 challenges associated with the hybrid low-cost PD solutions for the next-generation global navigation satellite system multi-carrier broadband waveform (GNSS-MCBBW). The focus of this Phase 2 effort is on the GNSS-MCBBW satellite transponder. The CSUF team was formed through the Industrial Project for Graduate Program in Applied Mathematics (IPGPAM), a joint collaboration project between CSUF and IFT. The CSUF team includes three CSUF faculty members serving as the CSUF principal investigator, the university lead, and the data science technical advisor, along with a graduate research assistant and a selected Graduate Student Team (GSTe). The CSUF-GSTe includes eight applied mathematics graduate students. This IPGPAM project focused on the advanced mathematical modeling and MATLAB simulation aspect of the non-ideal GNSS-MCBBW satellite system.

The research team has recently developed a new GNSS-MCBBW employing two onboard processing techniques, namely, HT and BPF. These processing techniques can generate single sideband GNSS-MCBBW (SSB-GNSS-MCBBW) waveforms that fit the spectrum within the L-band bandwidth of 500MHz. This paper discusses our modeling and simulation approach for the development and MATLAB implementation of a satellite system emulator that can accurately generate the proposed GNSS-MCBBW

[1] Graduate Student in Applied Mathematics, Lead MATLAB Implementer of the non-ideal Hilbert Transform system models, California State University in Fullerton (CSUF).

[2] Graduate Student in Applied Mathematics, Lead MATLAB Implementer of non-ideal Bandpass Filter system models, CSUF.

[3] Dr. Tien M. Nguyen is also with The Aerospace Corporation. He is a retired Engineering Fellow, Raytheon.

[4] Graduate Student in Applied Mathematics, Graduate Research Assistant, CSUF.

waveforms. The goal of this emulator is to provide a robust and flexible digital engineering (DE) platform that can be used to (i) evaluate the SSB-GNSS-MCBBW performance and (ii) perform alternative waveforms assessment in the presence of ideal and non-ideal hardware system components. For demonstration, this paper discusses the use of existing GPS L1, L2, and L5 waveforms along with the PCM/PSK/PM multi-carrier modulation technique with sinewave subcarriers.

The paper describes the emulator and discusses the impact of non-ideal hardware components on the proposed signals. The emulator is capable of simulating and evaluating the SSB-GNSS-MCBBW performances in terms of modulation losses and power spectral density (PSD) in the presence of AM-AM/AM-PM distortions. The distortions are caused by the high power amplifier (HPA) non-linearity. The HPA hardware model implemented in the emulator uses actual measured data for a typical L-band HPA.

An ideal HPA linearizer (a.k.a. HPA pre-distorter) model is also developed and implemented in the GNSS-MCBBW emulator to mitigate the impact of HPA non-linearity on the SSB signals. The ideal HPA pre-distorter (PD) model uses actual HPA-measured data to determine the amount of AM-AM and AM-PM distortions and compensate for them. The HPA model can be set at different input back-off power (IPBO) and three system operating temperatures 25°C, 27°C, and 30°C.

The non-ideal hardware models for a balanced modulator, a phase modulator, a reference satellite clock, an intermediate frequency-to-radio frequency (IF-to-RF) converter, and an RF filter implemented in our MATLAB emulator will be discussed in detail. The models implemented in the MATLAB emulator will allow the system designer to control the system hardware specifications (e.g., within specifications or out-of-specifications) and evaluate the impact of the hardware imperfections on the signals in a controlled manner. As an example, typical specifications for the balanced modulator model are the (i) phase cross-talk, α, expressed in terms of the allowable unsuppressed carrier component in decibels, and (ii) phase offset between the in-phase and quadrature-phase components within β milli-radians. Our balanced modulator model can simulate the impacts of α = -20 dB and β = +100 milli-radians on the modulated signal. Each of the hardware models used by the emulator was tested and verified using existing GPS specifications to ensure that the models provided the expected performance results.

Simulation results for both HT and BPF processing techniques with and without HPA PD will be presented for comparison purposes. The modulation losses and PSD simulation results were obtained for both within-specification and out-of-specification cases using the MATLAB-implemented hardware models. These will also be presented and discussed.

The paper is organized as follows: (i) Section 2 provides an overview of the proposed GNSS-MCBBW satellite system emulator, (ii) Section 3 presents the satellite system models for the non-ideal system components, (iii) Section 4 describes the MATLAB implementation approach and MATLAB models for the proposed non-ideal GNSS-MCBBW satellite system component models, (iv) Section 5 provides non-ideal satellite system simulation results, and (v) Section 6 concludes with a summary of the work done on the modeling and simulation of the non-ideal system components, future work, and way-forward.

2. Overview of the proposed GNSS-MCBBW Satellite System Emulator

Reference 1 provides a description of an end-to-end GNSS-MCBBW system. The satellite system emulator is derived from [1] and shown in Figure 2.1. This figure shows that the emulator can produce either Hilbert Transform (HT) GNSS-MCBBW signal or bandpass filter (BPF) GNSS-MCBBW signal. The HT GNSS-MCBBW signal is generated by selecting the switch on the blue path connected to the HT node. The BPF signal is produced by selecting the red path connected to the BPF node. As discussed in [1], both the

proposed HT and BPF techniques produce an upper single sideband (SSB) GNSS-MCBBW signal that fits the existing allocated L-band spectrum reserved for the GPS satellite system. In addition, the satellite system emulator also includes: (i) an HPA pre-distorter (PD) using ML-AI technology enabler, (ii) an HPA model using actual L-band HPA AM-AM/AM-PM data collected from an industry HPA supplier, and (iii) waveform adaptive processing module (WAPM). The WAPM is not the focus of this paper, and a description of WAPM can be found in [2]. In the following sections, non-ideal models of the satellite system component will be discussed.

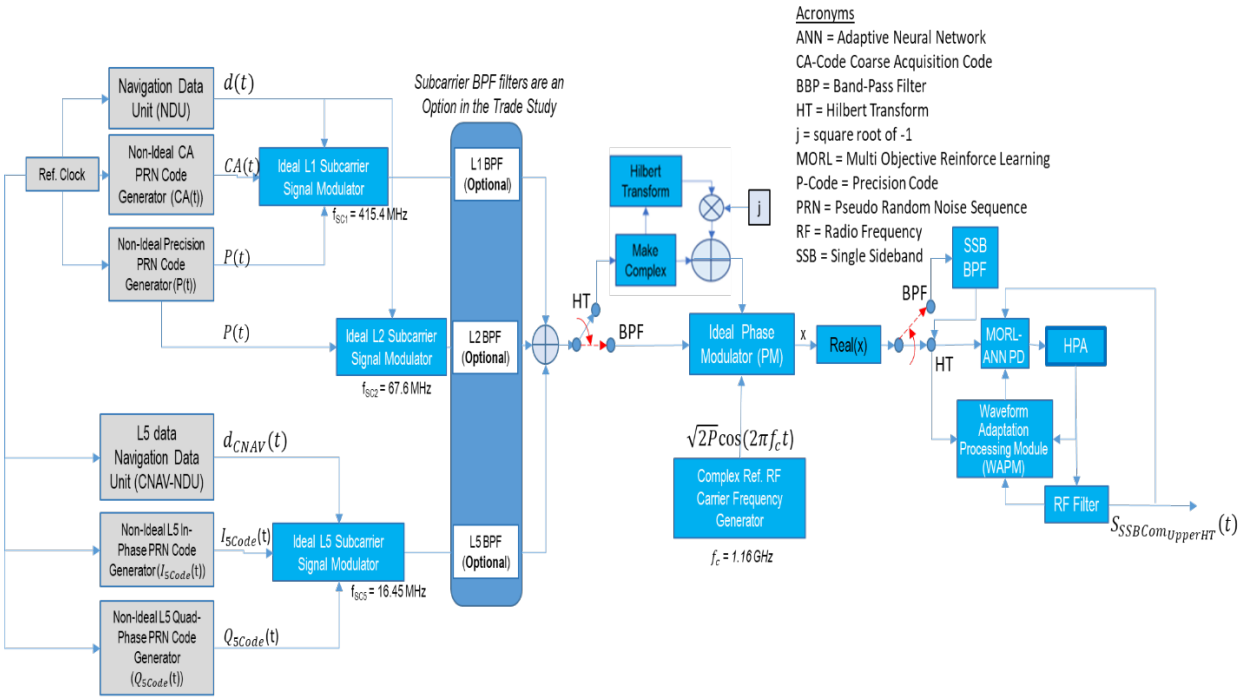

Figure 2.1: GNSS-MBBW Satellite System Emulator

3. Non-ideal Satellite System Models of the Proposed Emulator

This section describes the non-ideal models for the local oscillator (LO) timing clock drift of the satellite reference clock, intermediate frequency (IF) to radio frequency (RF) up-converter, LO phase noise, subcarrier modulator, IF-Band-Pass Filter (IF-BPF), phase modulator, High-Power Amplifier (HPA), and RF-BPF.

3.1. Non-Ideal PRN Code Generator Model

As shown in Figure 3.1, the LO random timing clock drift of $\Delta\tau$ of the satellite reference clock causes the imperfect (a.k.a. non-ideal) PRN code generator. Note that the red text (Req. No 7a, 7b) shown in Figure 3.1 indicates the clock drift specification for the proposed GNSS-MCBBW system that was derived from GPS specification. For within specification (a.k.a. In-Spec), the random variable $\Delta\tau$ is specified at 1 nanosecond, and it is assumed to be a uniformly distributed random variable between [a, b] seconds. The time drift range values “a” and "b" are chosen such that the average time error is ten nanoseconds.

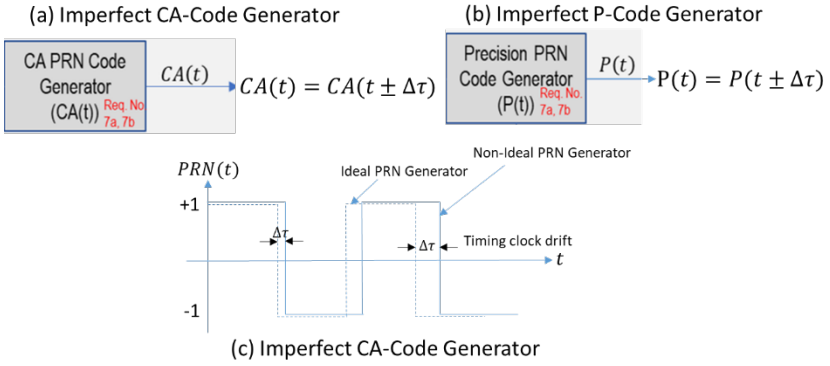

Figure 3.1: Non-Ideal PRN Code Generator Due to Clock Drift

3.2. Non-Ideal Up-Converter Model and LO Phase Noise Model

The non-ideal IF-to-RF up-converter model incorporates the imperfect effects when generating the reference signal and bandpass filtering (BPF), as shown in Figure 3.2. The imperfect reference signal includes the LO frequency error, Δf_{eRF}, LO phase noise, ϕ_P. The imperfect RF BPF model assumes the amplitude ripple is within 0.25 dB and the phase has a constant linear phase shift within the 3-dB passband bandwidth. The out-of-band specification for the RF-BPF requires a minimum of 40 dB suppression. Using GPS specification, the frequency error Δf_{eRF} is assumed to be uniformly distributed within [$-f_{eRF}$ f_{eRF}] with $f_{eRF} = 4.56710^{-10}.f_{RF}$, where f_{RF} is the RF frequency of the carrier signal. The phase noise is assumed to be Gaussian with zero mean and standard deviation of 0.1 RMS radian. The frequency error and phase noise are set outside of the GPS specification for the out-of-specification case.

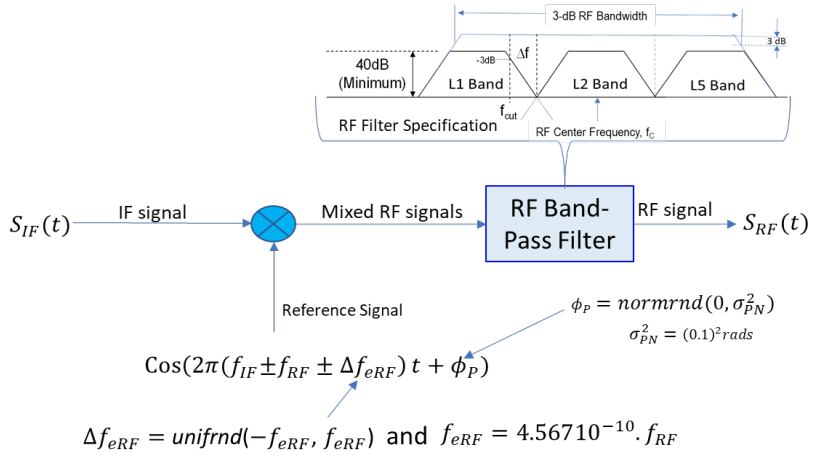

Figure 3.2: Non-Ideal Up-Converter Model

3.3. Non-Ideal Subcarrier Modulator Model

This section describes a non-ideal subcarrier modulator model derived in [3]. As discussed in 3, Figure 3(a) shows a perfect balanced modulator for an ideal signal generator of $A\cos(\omega_c t)$ and an input signal of $S(t)$, where A is the amplitude and ω_c is the angular carrier frequency. If the modulator gain is set to 1 and A is set at ½, the output of the ideal modulator is simply equal to $S(t)\cos(\omega_c t)$. Figure 3(b) shows an imperfect unbalanced modulator where the output is a function of the amplitude imbalance, Γ, and phase imbalance, θ. As shown in Figure 3(b), the output has two components, namely, a desired signal component, $S_D(t)$, and an undesired signal component, $S_U(t)$. The undesired signal component is also referred to as the

unsuppressed carrier component. For within specification (In-Spec), Γ and θ should be specified such that $\propto$ (dB) is less than or equal to -20 dB, where $\propto$ (dB) is defined as $10\log_{10}(\propto)$. Note that for an imperfect signal generator, the output of the generator will include the frequency drift and phase noise, as discussed in Section 3.2 above.

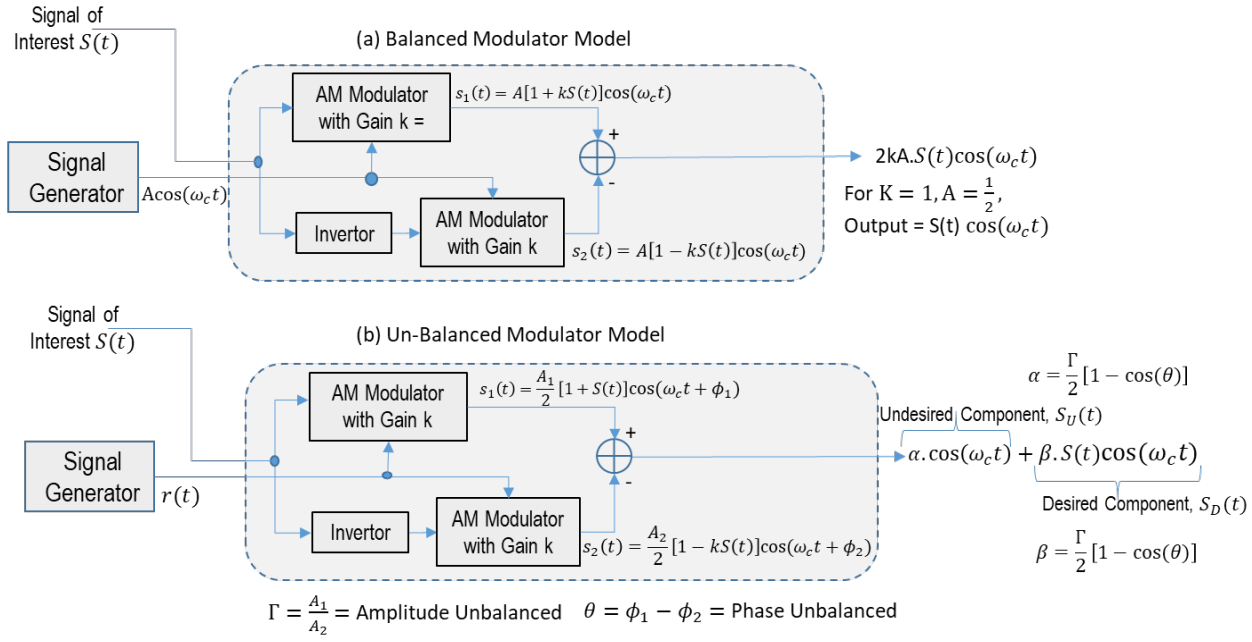

Figure 3.3: Balanced Modulator and Non-Ideal Unbalanced Modulator Models

3.4. Non-Ideal Phase Modulator Model

The non-ideal phase modulator (PM) includes a carrier generator and a non-linear processor with an input signal and an output signal. The carrier generator generates the sinusoidal carrier signal with an RF carrier frequency signal at f_c with a signal power level set at a value of P. As shown in Figure 3.4, the non-linear processor takes the input signal and places it in the phase of the sinusoidal carrier signal.

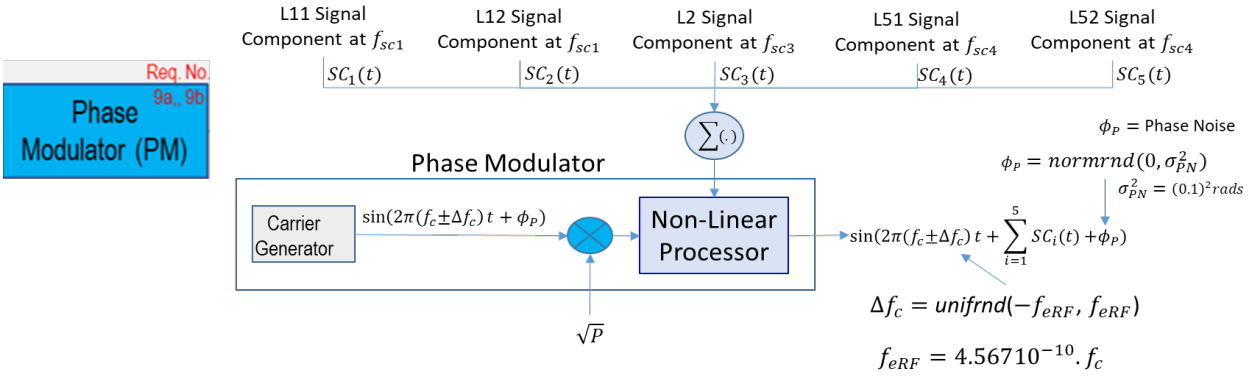

Figure 3.4: Non-Ideal Phase Modulator Model

The input to the PM model is the sum of the L1, L2, and L5 signal components. The output is assumed that the carrier generator is imperfect with a carrier frequency drift and a phase noise. For the In-Spec case, the carrier frequency drift, f_{eRF}, is equal to $4.56710^{-10} f_{RF}$, where f_{RF} is the RF frequency of the carrier signal,

and the phase noise, ϕ_P, is assumed to be Gaussian with zero mean and standard deviation of 0.1 RMS radian.

3.5. Non-Ideal HPA Model

The HPA model used in our satellite system emulator is similar to [4] and shown in Figure 3.5. This model uses the table look-up model by using actual measured Amplitude Modulation-to-Amplitude Modulation (AM-AM) and Amplitude Modulation-to-Phase Modulation (AM-PM) of an HPA at room temperature. In our emulator, we use the measured AM-AM/AM-PM data from an L-Band HPA supplier. For the non-ideal HPA model, we incorporate measured AM-AM/AM-PM data for various system temperatures other than room temperature. The detailed description and operation of this HPA model can be found in [4].

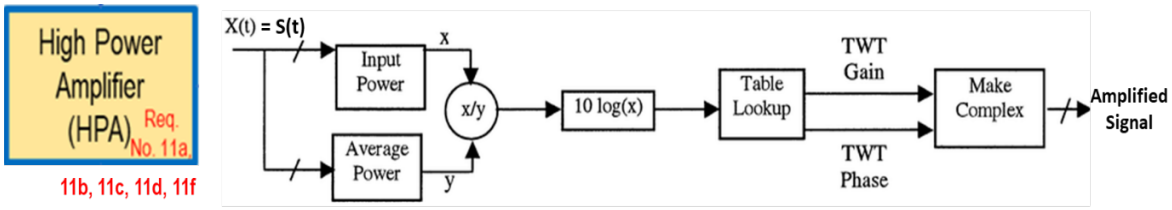

Figure 3.5: HPA Model

3.6. RF-BPF Model

The RF-BPF model is depicted in Figure 3.6. Following industry standards, the filter's passband is defined as the 3-dB bandwidth, and the stop band is defined as the band outside the passband. For the In-Spec case at room temperature, the passband ripple is to be less than or equal to 0.25 dB, and stop band attenuation is less than 40 dB. In our satellite system emulator, the RF-BPF model is assumed to be operating within specification.

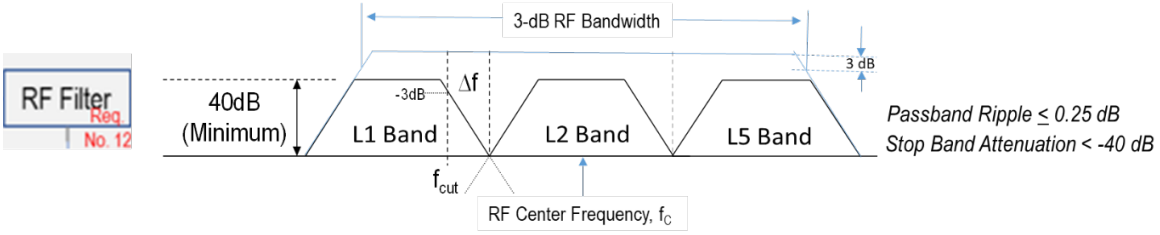

Figure 3.6: RF-BPF Model

4. MATLAB Implementation of the non-ideal System Component Models

The approach used to implement the non-ideal system components into MATLAB depended on the ideal model. The ideal system component model was further tweaked to match our non-ideal specifications. The first non-ideal MATLAB approach implemented is the Time Drift MATLAB model, which is necessary to create the non-ideal subcarrier modulator models. This leads to the non-ideal subcarrier models, where we again incorporate all the parameters defined previously that make up the non-ideal subcarrier modulator models. With the created subcarrier modulator models, the subsequent implementation is the non-ideal phase modulator, which again incorporates parameters previously defined. Then, we investigate the filters implemented throughout our code and then analyze the non-ideal HPA, where we cover the specifications for current GPS HPA.

Reference 5 is the final report submitted for meeting official IPGPAM requirements, which contains many of the results seen throughout Sections 4 and 5.

4.1 Time drift MATLAB Model

One of the first non-ideal system components we simulated is the time drift caused by the local oscillator. The average time difference between the chips on the same carrier should be at most ten nanoseconds. One of the significant challenges when simulating this time drift model was taking the existing ideal C/A PRN code or the Precision PRN code and moving the zero-crossings within those codes. More specifically, moving it in such a way that τ is uniformly distributed with parameters -10 and 30 nanoseconds is mimicked, considering that codes are represented as discrete vectors in MATLAB.

This function takes the generated ideal PRN P-Code or C/A code, and changes said code to simulate the timing drift. This function begins by looking for the instances that the P-code or the C/A code, depending on what our input is, crosses over zero with the built-in MATLAB function *diff*. As mentioned previously, our code is comprised of 1's and -1's; therefore, non-zero differences imply a crossing of the zero axis, specifically 2 when crossing from -1 to 1 and -2 when crossing from 1 to -1. We create the random variable τ, incorporate it in the number of samples per chip, and modify our inputted code to include the random variable τ. The code moves the zero crossing forward or backward to simulate the time drift, or in other words, the jittering caused by the satellite system's local oscillator. As will be shown when creating the non-ideal subcarrier modulator models, L1, L2, and L5 all use either the P-code or the C/A code, so part of creating the non-ideal subcarriers involves using these newly created non-ideal codes.

4.2 Non-ideal MATLAB Model for Subcarrier Modulator Models

Figure 4.1 demonstrates the modulation of the L11 and L12 signals, which will be used to simulate the L1 signal. Below are the mathematical models of the non-ideal subcarrier modulator models for L11, L12, L2, L51, and L52, which we implemented in MATLAB.

L11 and L12 subcarrier components at the output of L1 unbalanced modulator:

$$SC_1(t) = \alpha\cos(2\pi(f_{sc1} \pm \Delta f_{e1})t) + \beta A_1 m_1 CA(t \pm \Delta\tau)d(t)\cos(2\pi(f_{sc1} \pm \Delta f_{e1})t) \quad (1)$$

$$SC_2(t) = \alpha\sin(2\pi(f_{sc1} \pm \Delta f_{e2})t + \phi_{e2}) + \frac{\beta}{\sqrt{2}}A_1 m_1 P(t \pm \Delta\tau)d(t)\sin(2\pi(f_{sc1} \pm \Delta f_{e2})t + \phi_{e2}) \quad (2)$$

$$f_{sc1} = f_{sc2} = 1575.42E6 - f_c\,,\ \Delta f_{e2} = \Delta f_{e1}\,. \quad (3)$$

L2 subcarrier component at the output of L2 unbalanced modulator:

$$SC_3(t) = \alpha\cos(2\pi(f_{sc3} \pm \Delta f_{e3})t + \phi_{e1}) + \beta A_3 m_3 P(t \pm \Delta\tau)d(t)\cos(2\pi(f_{sc3} \pm \Delta f_{e3})t + \phi_{e3}) \quad (4)$$

$$f_{sc3} = 1227.60E6 - f_c \quad (5)$$

L51 and L52 subcarrier components at the output of L5 unbalanced modulator:

$$SC_4(t) = \alpha\cos(2\pi(f_{sc4} \pm \Delta f_{e4})t) + \beta A_4 m_4 P(t \pm \Delta\tau)d(t)\sin(2\pi(f_{sc4} \pm \Delta f_{e4})t) \quad (6)$$

$$SC_5(t) = \alpha\sin(2\pi(f_{sc4} \pm \Delta f_{e4})t + \phi_{e5}) + \beta A_5 m_5 P(t \pm \Delta\tau)d(t)\cos(2\pi(f_{sc4} \pm \Delta f_{e4})t + \phi_{e5}) \quad (7)$$

$$f_{sc4} = f_{sc5} = 1176.60E6 - f_c \quad (8)$$

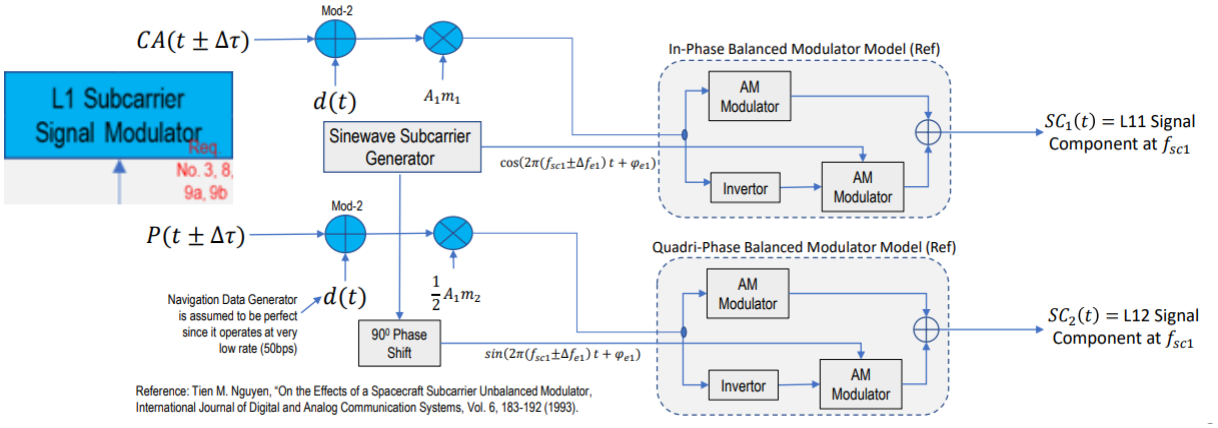

Figure 4.1: Non-ideal L11 and L12 Subcarrier Components

The MATLAB implementation of these non-ideal subcarriers is straightforward, with key parameters defined within the MATLAB code according to the GPS specifications. In our model, the RF carrier, f_c, is set at 1.16 GHz. As previously stated, this code implements the non-ideal components that create the subcarrier models. Including within the subcarrier models is the time drift or jitter model, which was previously mentioned above. Using equation (1) and L1 for demonstration, the key parameters that create the non-ideal subcarriers include the frequency error Δf_{e1} and Δf_{e2}; the phase imbalance ϕ_1 and ϕ_2; α and ß, which are defined by the amplitude imbalance Γ and phase imbalance θ; A1 and A2, and the modulation indices m_1 and m_2. Here, we have $A_2 = \frac{A_1}{\sqrt{2}}$, since L12 has half the power of L11. The frequency error Δf_{e1} is defined as being uniformly distributed between $-f_{e1}$ and f_{e1}, where $f_{e1} = 4.5670 * 10^{-10}$ multiplied by the subcarrier frequency for L1: SC_L1. Here, we have the difference between the L1 and the carrier frequency of the MCBBW as SC_L1. This is equivalent to a change in the P-code chipping rate of 10.23 MHz to 10.229999995426 MHz. Similar results for f_{e2} and Δf_{e2}. Here, we have the phase imbalance ϕ_1 equal to 0, and ϕ_2 defined to have gaussian distribution with a mean of 0 and a standard deviation of 100 milliradians. The m_i's are defined as the modulation indices of the system. For both L2 and L5, they share similar key parameters, the only difference being the index of the parameters and their frequencies.

4.3 Non-ideal MATLAB Model for Phase Modulator

The next system component that we will be focusing on is the phase modulator. In order to incorporate non-ideal effects into the phase modulator, we will be incorporating frequency errors and the phase noise, defined by Δf_c and Φ_{pm}, respectively. We define Δf_c as being uniformly distributed with lower bound $-f_{ec}$ and upper bound f_{ec}, which is defined as the frequency carrier, 1.16 GHz, multiplied by $\frac{\Delta f_c}{f_c} = 4.567\text{e} - 10$. The distribution for the phase noise, Φ_{pm}, is normally distributed with mean 0 and variance 0.01 radians. This model is a straightforward approach to simulate our specifications. The following is the general formula for our non-ideal phase modulator:

$$S(t) = \sqrt{2}\cos(2\pi(f_c \pm \Delta f_c)t + \Sigma_{i=1}^{5} SC_i(t) + \Phi_{pm}) \quad (9)$$

where SC_i consists of the subcarrier frequencies L11, L12, L2, L51, and L51 listed in the previous section.

4.4 Non-ideal MATLAB Model for Filters

For the baseline bandpass filter model, we select a bandwidth for L1, L2, and L5 of 30.69 MHz or 20.46 MHz; we choose 20.46 MHz as the baseline. An ideal filter would perfectly filter out the undesired frequencies, leaving only a bandwidth of desired frequencies around L1, L2, and L5. Our bandpass filter has an allowable correlation loss between 0.3 and 0.6 dB which is due to the space vehicle modulation and filtering imperfections. The RF filter's limit on the in-band spurious transmissions is -40 dBc from the Space Vehicle; that is, the in-band spurious transmission should not exceed -40 dBc over each of the respective bands. The passband ripple should be less than 0.25 dB. For our code, the bandpass filter had steepness between 0.85 to 0.999, and the frequency determined a passband filter range we were interested in, whether it be L1, L2, L5, or the carrier frequency.

4.5 Non-ideal HPA MATLAB Model

The HPA for the existing GPS has a gain between 51 dBm and 55 dBm while operating at 250 Watts. The operating frequency is at L1 = 1575.42 MHz, L2 = 1227.60 MHz, and L5 = 1176 MHz, with a bandwidth 20.46 MHz or 30.69 MHz. We use 20.46 MHz in our case. The maximum AM/PM conversion is less than 2 degrees per dB at linear input power. We use a look-up table and operate at varying temperatures: 25°C, 27°C, and 30°C. Our Satellite system will take two approaches to create the single Upper Side Band: Hilbert Transform and Bandpass Filter. Our goal will be to take these two approaches and compare how the non-ideal signal performs compared to the ideal signal. We will be doing this by calculating the power spectral density (PSD) of both our ideal and non-ideal signals and then plotting these against each other. The figure below is a summary of the two approaches for our system.

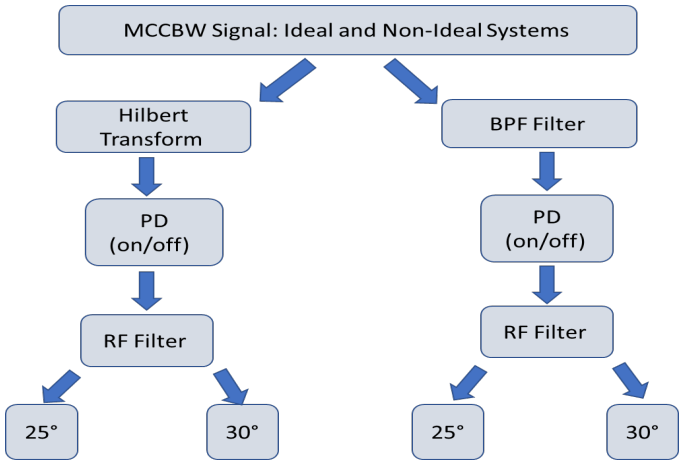

Figure 4.2: MCBBW Signal approaches for the Single Upper Side Band

Either the Hilbert Transform or the BPF Filter will be applied to our non-ideal MCBBW signal, which is the output from our non-ideal phase modulator. Then we will choose whether or not to

apply the pre-distorter, apply the RF Filter, and finally look at modulation losses for ideal and non-ideal signals at -27 dB and -6 dB at 25°C and 30°C.

Below, in Figure 4.3, we can see which values of Γ and θ satisfy the equation

$$\alpha(dB) = 20\,log10(\alpha) \leq -20\ \text{dB}.$$

As stated before, the α term is the coefficient of the unsuppressed carrier component, which controls the signal loss and the spurious emission due to the imperfect satellite system components. The values of blue satisfy the given equation above. From the plot, we can see that the parameter with the bigger influence is Γ. For the most part, if Γ ≥ 0.8, the equation is satisfied. Physically, this corresponds to the amplitude imbalance having a value above 0.8. Once that is achieved, the phase imbalance can take any value between 0 and 10 degrees for the most part.

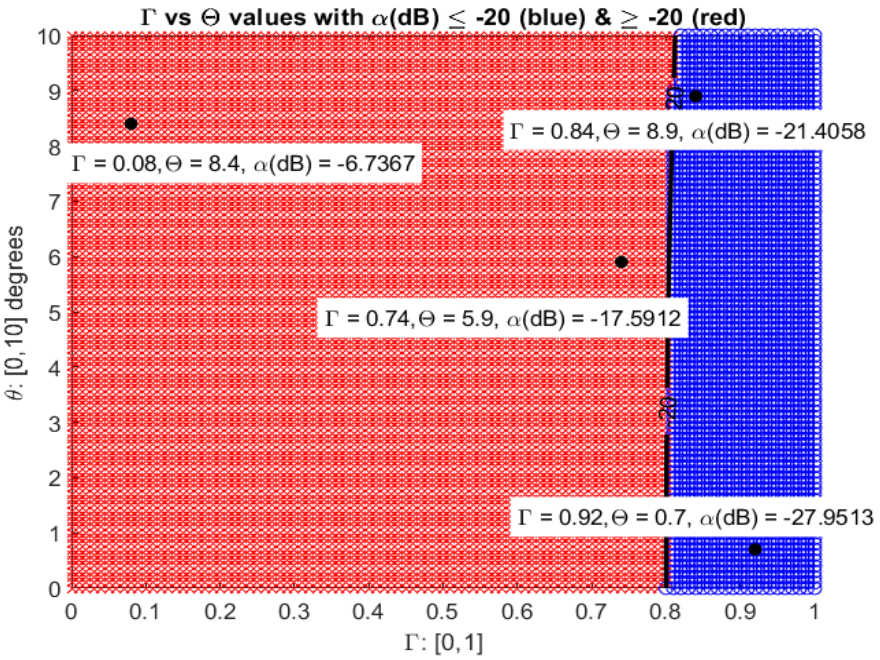

Figure 4.3: Out-of-spec (red) and in-spec (blue) Values of α with Varying Γ and θ

We wanted to compare the PSDs of the L11 subcarrier with values α(dB) = -27.9 dB (Figure 4.4) and α(dB) = -6.7 dB (Figure 4.5). Clearly, we can see that ideal and non-ideal signals are more closely related when the α(dB) term is within spec, as opposed to Figure 4.5, where the out-of-spec α(dB) value caused much more distortion in the signal. We see the unsuppressed carrier component having a much greater influence on the signal when out-of-spec [5]. Note: We see similar results to the other carrier components L12, L2, L51, and L52.

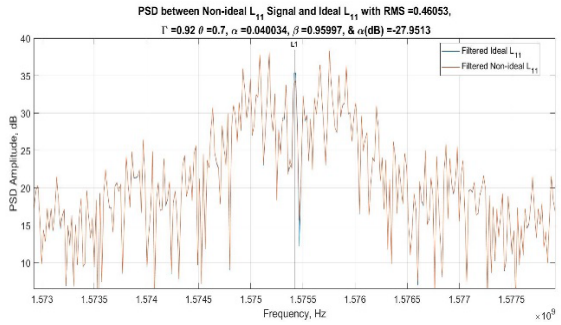

Figure 4.4: PSD L11 ideal vs. non-ideal, α(dB) = -27.9 dB

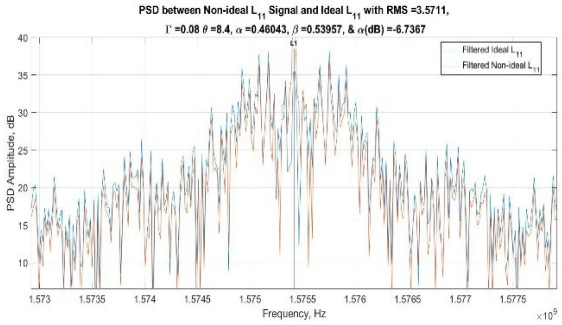

Figure 4.5: PSD L11 ideal vs. non-ideal, α(dB) = -6.7 dB

Figures 4.6 and 4.7 show the timing error caused by the unsuppressed carrier. We can see that, after the signal has been modulated, there is a timing error seen in both cases due to the red being non-ideal and the blue signal being an ideal MCBBW signal. On the right, the timing error is larger and appears sooner as opposed to the left, where the timing error isn't immediately apparent.

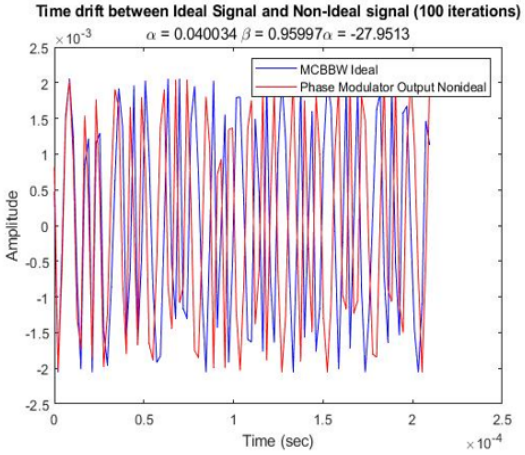

Figure 4.6: Timing Drift ideal and non-ideal signal, α(dB) = -27.95

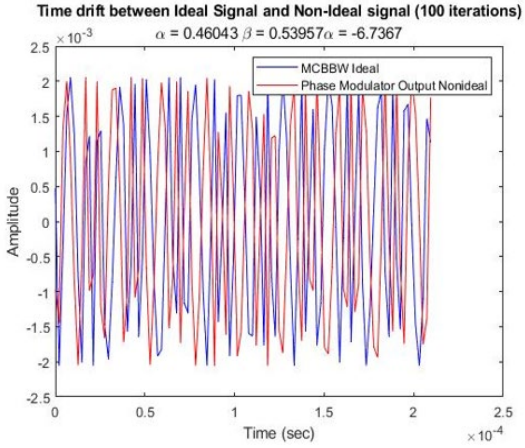

Figure 4.7: Timing Drift ideal and non-ideal signal, α(dB) = -6.73

5. Non-ideal System Simulations Results

This section presents non-ideal system simulation results for both HT and BPF signal processing approaches under various imperfect operating conditions.

5.1 MATLAB Simulations and Evaluation Results for HT

The first approach used to generate the single upper sideband is the HT. This approach consists of applying the HT to both the ideal and non-ideal MCBBW signals. To see the effects that the non-ideal components have on the signal, we will plot the PSD of both the ideal and non-ideal signals and compare these. We will be examining the effects of the non-ideal satellite system components for the case when the non-ideal signal is out of the required specifications, or α(dB) = -6.74 dB. Additionally, we will be evaluating the performance of this signal at various operating temperatures (25°C, 27°C, 30°C). Recall that the non-ideal components that have been

incorporated into the system are the non-ideal clock, non-ideal subcarrier modulator, and non-ideal phase modulator. Figure 5.1 below displays the power spectral density (PSD) of the ideal signal (blue) and the non-ideal signal (red) after using the Hilbert Transform but before it has passed through the High-Power Amplifier (HPA). This signal will be referred to as the Pre-HPA signal. We can see that there is some distortion in the non-ideal signal and more spikes at undesired frequencies. That is, there are spurious emissions in the PSD caused by imperfections, or non-ideal components, in the signal. First, focusing on the L2 and L5 frequencies, we can see that there are spurious emissions between L5 and L2 that range approximately between 30 dB and 50 dB in amplitude. Additionally, around L1 we can see that spurious emissions to the right reach an amplitude of 40 dB.

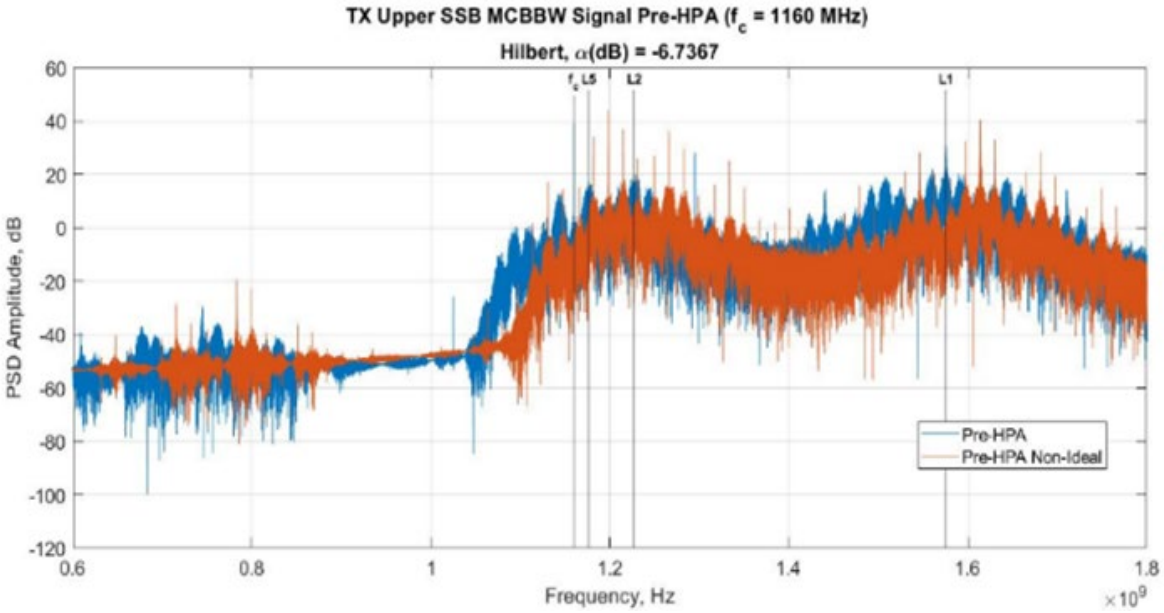

Figure 5.1: PSD of Pre-HPA signal with Hilbert Transform

After the Hilbert Transform is applied to the non-ideal MCBBW signal, the signal will pass through the HPA and then finally through the RF Filter. However, we will examine two cases, the case where the pre-distorter is applied before the signal passes through the HPA and the case where it is not. This will be done at the operating temperatures previously mentioned. Additionally, as stated, we will be examining the modulation losses in terms of percentages compared to theoretical values in the cases where we do and do not apply the ideal pre-distorter and present a visual representation of this by plotting bar graphs. It is important to note that the goal is not to optimize but rather to build an emulator with the capability to simulate the newly proposed MCBBW system. Below is the table for our results.

The modulation loss percentages were found by comparing the theoretical values to the actual values found. This is done by finding the normalized power of the signal of interest and subtracting that from the theoretical power of each signal. Equation 10 shows the equation used to find the theoretical values of the modulation losses, where J_n represents the Bessel function of the nth kind, and m_i's are the modulation indices, as seen in [1].

$$PSD_{L11}(f)/P = \frac{2}{16}\underbrace{[2J_1(m_2)J_0(m_2)J_0(m_3)J_o(m_4)J_0(m_4)]^2}_{\text{Modulation Loss Term for L11 component}}\left\{\begin{matrix}\left[\frac{\sin(\pi(f-(f_c+f_{SC2}))T_{C_1})}{\pi(f-(f_c+f_{SC2}))T_{C_1}}\right]^2+\left[\frac{\sin(\pi(f+(f_c+f_{SC2}))T_{C_1})}{\pi(f+(f_c+f_{SC2}))T_{C_i}}\right]^2+\\ \left[\frac{\sin(\pi(f-(f_c-f_{SC2}))T_{C_1})}{\pi(f-(f_c-f_{SC2}))T_{C_1}}\right]^2+\left[\frac{\sin(\pi(f+(f_c-f_{SC2}))T_{C_1})}{\pi(f+(f_c-f_{SC2}))T_{C_1}}\right]^2\end{matrix}\right\} \quad (10)$$

Simulation results of the modulation loss in Percentages (%) for signal in-spec and out-of-spec with and without ideal pre-distorter at 25°C, 30°C using HT are summarized in Table 5.1.

Modulation Losses (%) for f_c , L1, L2, L5 Compared to Theoretical Values–Hilbert Transform					
Non-Ideal α(dB) = -27.95 dB			Non-Ideal α(dB) = -6.74 dB		
	Without Pre-distorter	With Pre-distorter		Without Pre-distorter	With Pre-distorter
	25°C	25°C		25°C	25°C
	(%)	(%)		(%)	(%)
f_c	13.75	13.83	f_c	12.60	12.49
L1	18.21	18.01	L1	18.73	18.68
L2	0.00	0.00	L2	0.00	0.00
L5	9.33	9.39	L5	8.83	8.77
	30°C	30°C		30°C	30°C
fc	14.79	13.83	fc	14.09	12.49
L1	18.61	18.01	L1	18.92	18.68
L2	0.00	0.00	L2	0.00	0.00
L5	9.88	9.39	L5	9.58	8.77

Table 5.1: Summary of Modulation Loss in Percentages (%) for Signal in and out-of-spec with and without ideal pre-distorter at 25°C, 30°C using HT

First, we examine the case where the pre-distorter will be applied to the non-ideal signal before it passes through the HPA. Figure 5.2 (left) displays the modulation losses in percentages compared to theoretical values for the signal with α(dB) = - 6.74 dB at 25°C, 27°C, and 30°C and shows that with the pre-distorter, the modulation losses remain the same for all three temperatures. For the carrier, our modulation losses were 12.49% for all three temperatures, and for L1 they were 18.68% for all three temperatures for L2 they were neglectable. Note that the modulation losses for L1 and L5 are non-zeros due to the I/Q inter-channel interferences, whereas L2 has only one component [1].

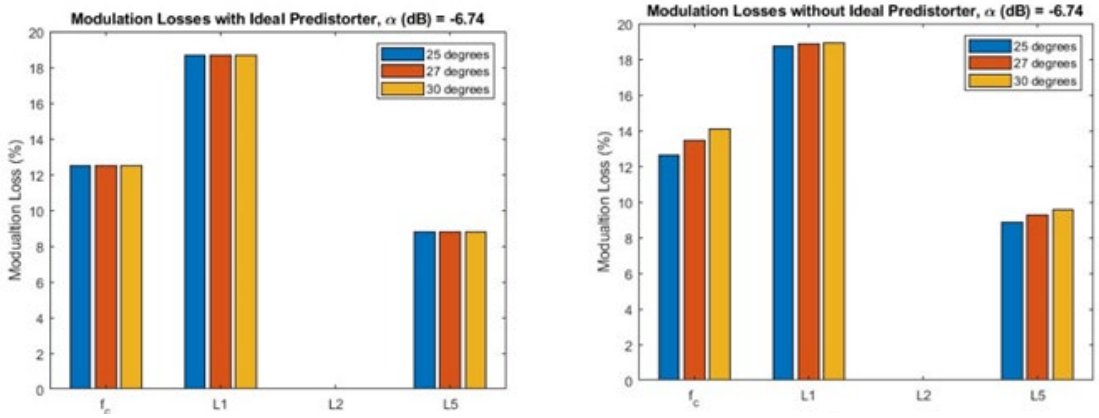

Figure 5.2 Modulation Losses (%) Compared to Theoretical Values, α(dB) = -6.74dB at 25°C, 27°C, and 30°C, with pre-distorter (left) without pre-distorter (right) using Hilbert Transform

In the case where the pre-distorter is not applied before the HPA, Figure 5.2 (right) displays a slight discrepancy in the modulation losses. Notice also that the modulation losses increase slightly as the operating temperature increases. For the carrier, the modulation losses are 12.60% and 14.09% for 25°C and 30°C, respectively. Also, for L1, the modulation losses are 18.73% and 18.92% for 25°C and 30°C, respectively.

Next, in Figure 5.4, below to the right, we examine the differences in modulation losses between the non-ideal signal that is within the specification (blue) and the non-ideal signal that is outside of the specification (red) when compared to the theoretical model with the pre-distorter. As seen in the figure, for the carrier and for L5, the modulation loss is higher for the signal that is within the specification. For L1, the modulation loss is slightly higher for the signal out-of-spec, and for L2, the modulation loss for both is essentially zero. These results are similar without the pre-distorter (Figure 5.4 left) since, for each non-ideal signal, the modulation losses with and without the pre-distorter are within one percent. Note that this graph displays results only for 25°C; however, these results remain consistent for other temperatures. This is evident in Table 5.1, which displays modulation losses for the non-ideal signal in and out-of-spec (α(dB) = -27.95 dB and α(dB) = -6.74 dB) at 25°C and 30°C.

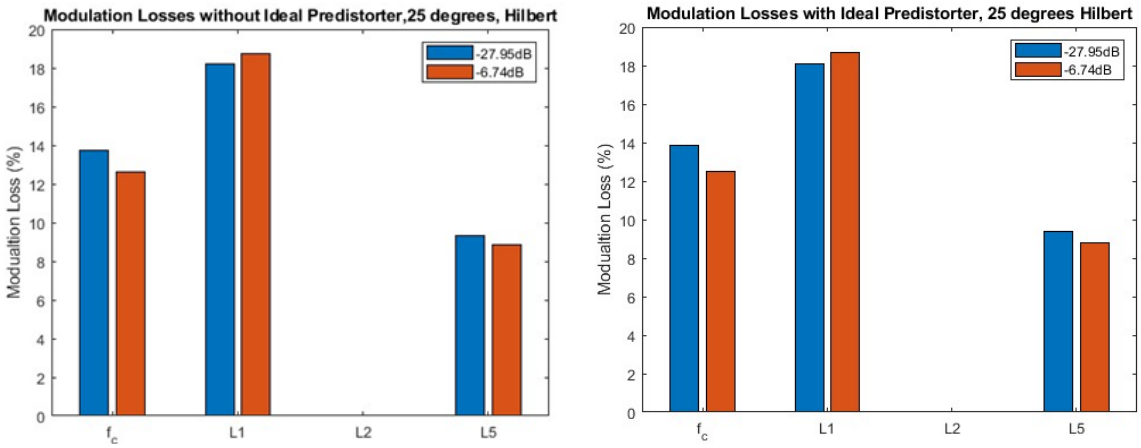

Figure 5.4: Comparison of Mod Loss (%) for non-ideal signal in (blue) and out-of-spec (red) at 25°C with PD (right) and without PD (left) using the Hilbert Transform

Finally, in order to evaluate the satellite system performance using the non-ideal signal and to identify the effects of the non-ideal components, we use a PSD plot and examine the discrepancies between the signal operating in and out-of-spec. This is shown in the figures below. Note that these figures show the signal (in-spec Figure 5.5, out-of-spec Figure 5.6) with the pre-distorter that has passed through the HPA and the RF filter.

Figure 5.5 shows the PSD of the non-ideal signal operating within spec (red) against the PSD of the ideal signal (blue), while Figure 5.6 shows the PSD of the non-ideal signal operating out-of-spec (red) against the PSD of the ideal signal (blue). It is evident that we see more distortion in the non-ideal signal with an α(dB) value that is out-of-spec. This is evidenced by the fact that we see

more spurious emissions along the MCBBW signals at frequencies that are not our L bands of interest. Specifically, between the L5 and L2 frequencies, as before, there are spurious emissions that reach an amplitude ranging from 30 dB to 50 dB. Moreover, we also find that the L1 signal has been suppressed, as demonstrated by the red curve having a lower amplitude than the ideal blue signal at the L1 frequency.

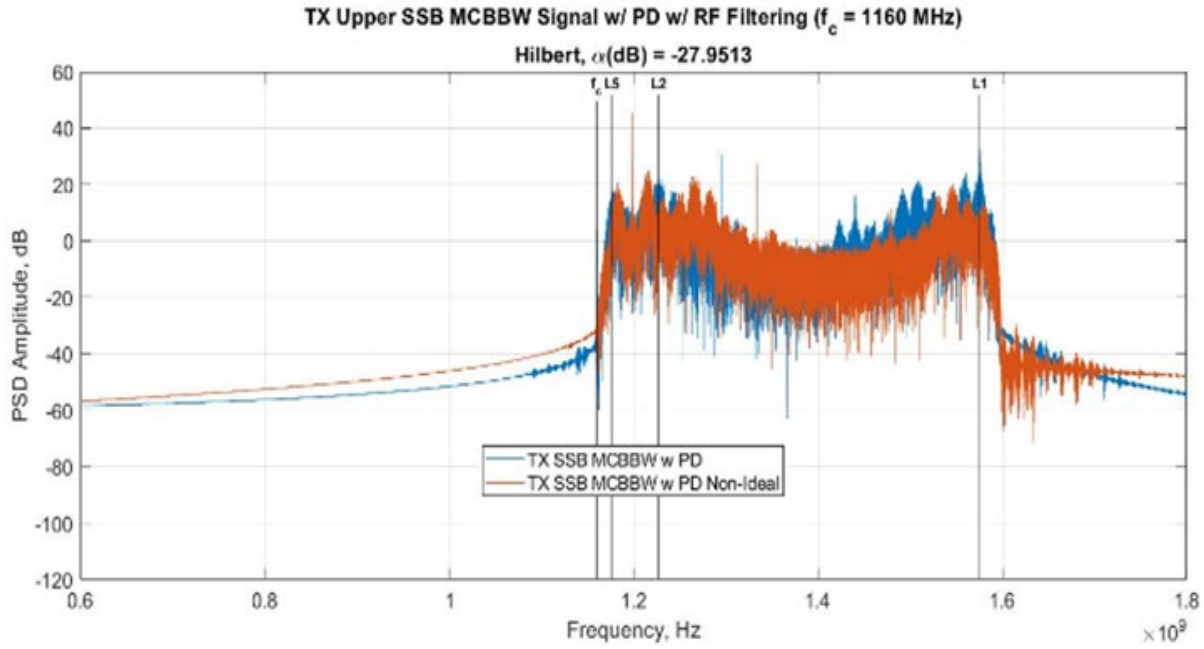

Figure 5.5: PSD of ideal and non-ideal MCBBW Signals with PD and with RF Filtering, α(dB) = -27.95 dB, using the Hilbert Transform

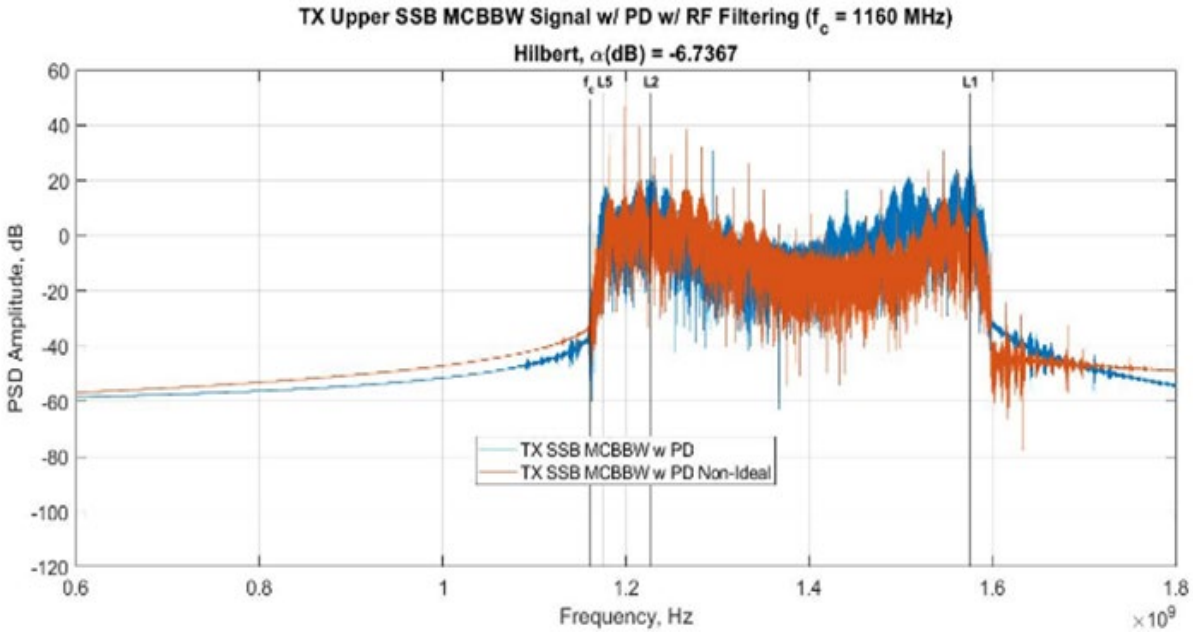

Figure 5.6: PSD of ideal and non-ideal MCBBW Signals with PD and with RF Filtering,

α(dB) = -6.7367 dB

Finally, we also aimed to compare the non-ideal signal at different operating temperatures; we do this by comparing the PSD of the signal at different temperatures. In Figure 5.7, we see that for all three temperatures in consideration, there are not a lot of discrepancies between the signals. For all three temperatures, we see spurious emissions through our signal, particularly close to the L5 and L2 bands. Additionally, we continue to observe the L1 suppression due to imperfections for all three cases. However, we do note that for the case where we operate at 30°C, some of the spikes in PSD are of a slightly higher amplitude though this discrepancy is not very significant.

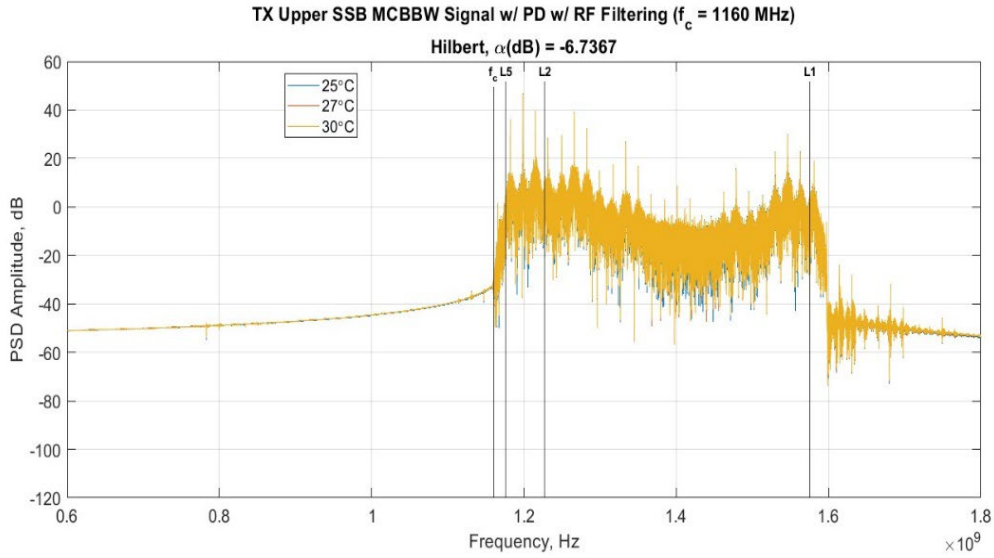

Figure 5.7: Non-ideal (α(dB) = -6.74dB) MCBBW Signal at 25°C,27°C, 30°C

5.2 MATLAB Simulations and Evaluation Results for BPF

The second approach used to generate the single upper sideband is the BPF approach. We applied the BPF to both the ideal and non-ideal MCBBW signal (signal with α(dB) operating in and out-of-spec). Then, as with the Hilbert approach, we will evaluate the satellite system performance by calculating the modulation losses compared to the analytical model and by plotting the PSD. This is done for various operating temperatures (25°C, 27C°, 30°C). Figure 5.8 displays the signal that is out-of-spec (α(dB)=-6.74dB) after the Bandpass Filter has been applied. We can see that similar to the Hilbert approach, there are spurious emissions throughout our signal, particularly near the L5 and L2 bands; as with the Hilbert Transform, we can see that these spurious emissions amplitudes are approximately between 30 dB and 50 dB. There are also spurious emissions near the L1 band; the second spike to the right has an amplitude of approximately 40 dB. In addition to this, we can also see suppression of the L1 frequency due to the signal imperfections that were incorporated into the development of the non-ideal signal (non-ideal clock, non-ideal subcarrier modulator, non-ideal phase modulator).

Moreover, as was the case with the Hilbert Transform, we looked at two cases within the Bandpass Filter Approach. The case where we apply the pre-distorter before the HPA and the case where the pre-distorter is not applied at different operating temperatures. To evaluate the system performance

for each case, we calculated the modulation losses in percentages compared to the theoretical values, as seen in Table 5.2. As a reminder, it is important to note that the goal is not to optimize but rather to build an emulator with the capability to simulate the newly proposed MCBBW system.

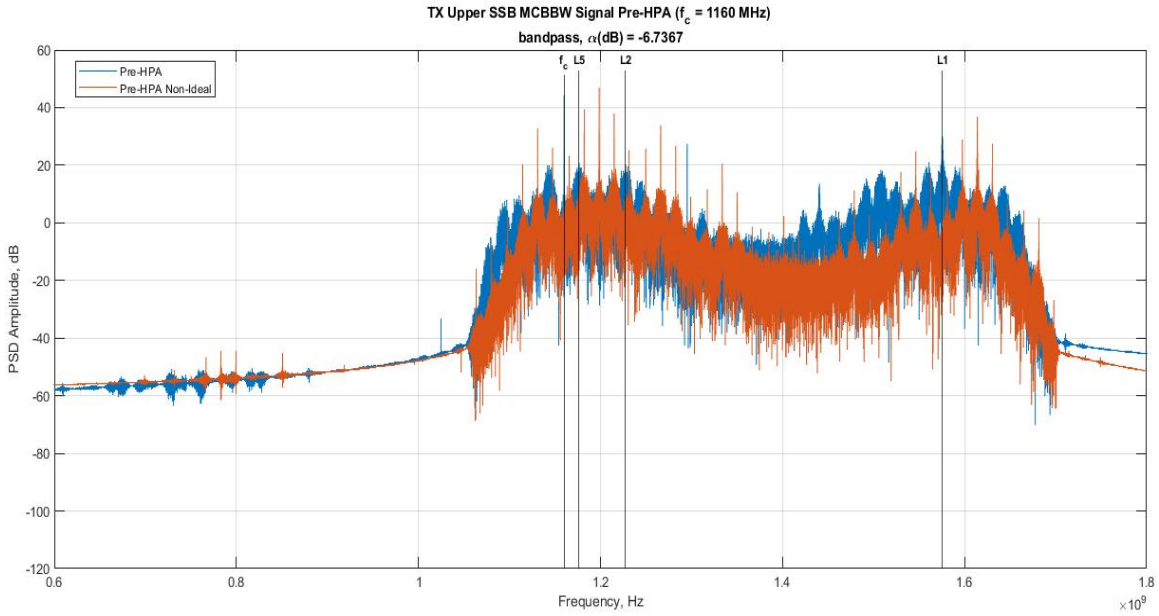

Figure 5.8: PSD of Pre-HPA signal with α(dB)= -6.74dB using Bandpass Filter

Modulation Losses (%) for f_c , L1, L2, L5 Compared to Theoretical Values–Bandpass Filter					
Non-Ideal α(dB) = -27.95 dB			Non-Ideal α(dB) = -6.74 dB		
	Without Pre-distorter	With Pre-distorter		Without Pre-distorter	With Pre-distorter
	25°C	25°C		25°C	25°C
	(%)	(%)		(%)	(%)
f_c	6.50	6.13	f_c	5.35	5.10
L1	18.51	18.55	L1	18.97	18.98
L2	0.00	0.00	L2	0.00	0.00
L5	4.73	4.50	L5	4.29	4.15
	30°C	30°C		30°C	30°C
fc	10.38	6.13	fc	9.67	5.10
L1	18.79	18.55	L1	19.07	18.98
L2	0.00	0.00	L2	0.00	0.00
L5	7.08	4.50	L5	6.81	4.15

Table 5.2: Summary of Modulation Losses in Percentages (%) for Signal in and out-of-spec at 25°C, 30°C

Following Figures 5.9 and 5.10 display the comparison of the modulation losses (%) with the theoretical values for α(dB) = -6.74dB at 25°C, 27°C, and 30°C for the BPF approach. In Figure 5.9, we applied the pre-distorter to the signal with α(dB) = -6.74 dB, meaning that it is out-of-spec and will have more distortion than our non-ideal signal. We can see that the modulation losses remain the same for all three operating temperatures (25°C, 27°C, 30°C). We also note that we

have the highest modulation losses for the L1 frequency and almost zero loss in modulation for the L2 frequency in both approaches. Additionally, when compared to the Hilbert Transform, the modulation losses for the Bandpass Filter approach are smaller for the carrier frequency f_c and for L5, as it is shown in Table 5.2.

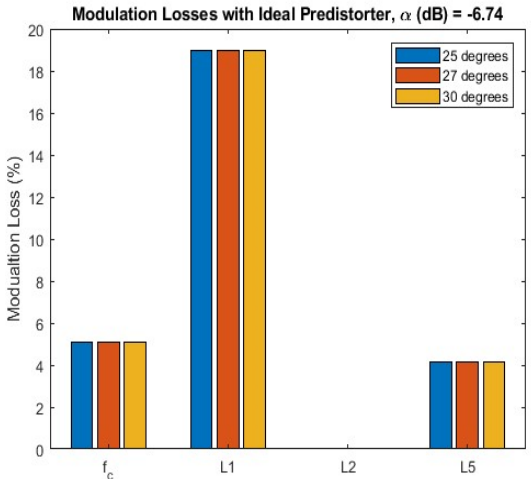

Figure 5.9: MCBBW Signal with ideal PD

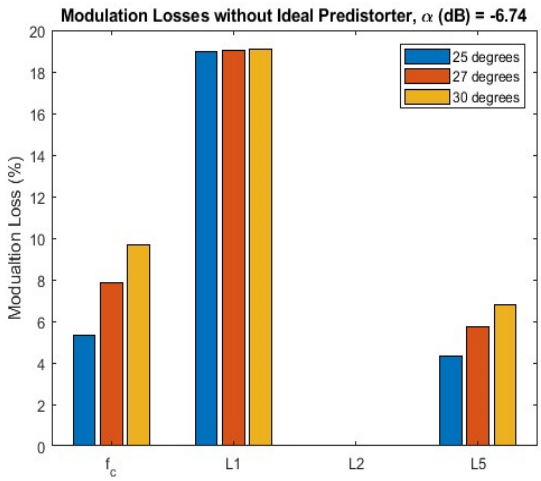

Figure 5.10: MCBBW Signal without ideal PD

In Figure 5.10, we see that without the pre-distorter, the signal modulation losses increase as the operating temperature increase. This increase in the percentage of modulation losses is more significant for the carrier frequency and L5 signal, while for L2, they are almost zero. Moreover, L1 has the highest modulation losses; however, while these do increase, the difference between the temperatures is not significant. For the carrier frequency, f_c, the modulation losses are 5.35% and 9.67% for 25°C and 30°C, respectively, without the pre-distorter and when out-of-spec. For L1, the modulation losses are 18.97% and 19.07% for 25°C and 30°C, respectively, without the pre-distorter and out-of-spec. Notice that the differences in modulation loss percentages at different operating temperatures for L1 and L5 are more pronounced at around 2 percent compared to the Hilbert Transform, where the operating temperature only affected the modulation losses with a less than one percent difference between them for the carrier frequency and L5.

Next, in Figure 5.11 (right), we examine the differences in modulation losses between the non-ideal system components with α(dB) = −27.95 dB (blue) and α(dB)=-6.74 dB (red) when compared to the theoretical model with the pre-distorter. Like the Hilbert Transform, for the carrier frequency and for L5, the modulation loss is higher for the signal that is within the specification. For L1, the modulation loss is higher for the signal out-of-spec, and for L2, the modulation losses for both α values are practically zero. These results are similar without the pre-distorter (Figure 5.11, left). Note that this graph displays results only for 25°C; however, the results remain consistent for other operating temperatures. Moreover, we can see that while these results have the same trends as the Hilbert Transform, the modulation losses percentages for the BPF approach are smaller than that of the Hilbert Transform, particularly for the carrier frequency and L5 subcarrier.

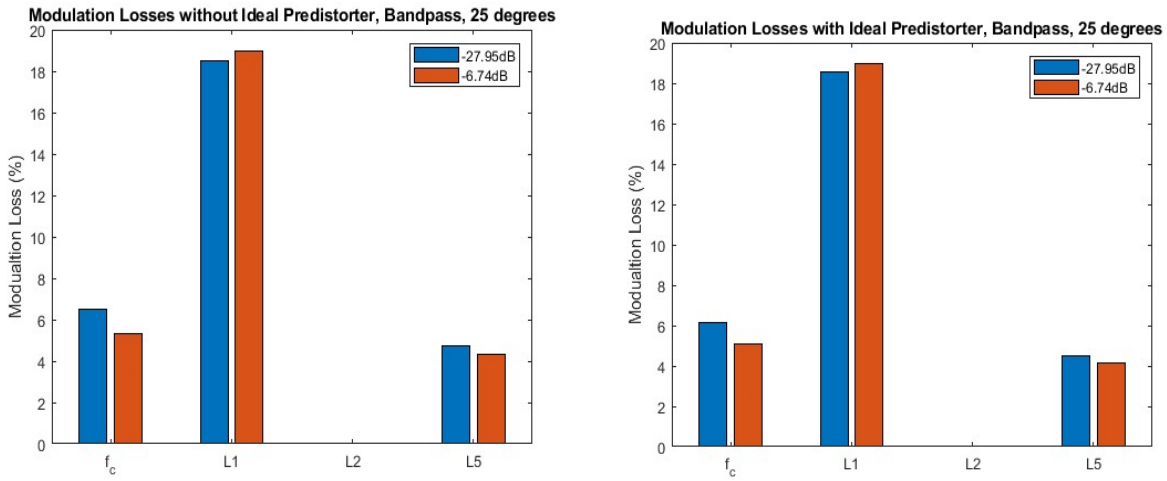

Figure 5.11: Comparison of Mod Loss (%) for non-ideal signal in (blue) and out-of-spec (red) at 25°C with PD (right) and without PD (left) using the Bandpass filter

Finally, as seen with the Hilbert transform, we compare the PSD of the satellite system using the Bandpass filter approach. We obtain similar results as with the Hilbert transform. We can see the differences in Figures 5.12 and 5.13 that occur when our signal is operating with non-ideal parameters that are within spec and outside of the spec, respectively. As we can see, there are a lot more spikes forming around Figure 5.13 when the α parameter is way out-of-spec. Comparing Figure 5.12 and Figure 5.13, around the L2 band we see more of the spikes in the immediate surroundings with a higher α value, as opposed to Figure 5.12 with a lower α value. We still see a few spikes when α(dB) = -27.95 dB, but significantly fewer spikes than when α(dB) = -6.7 dB.

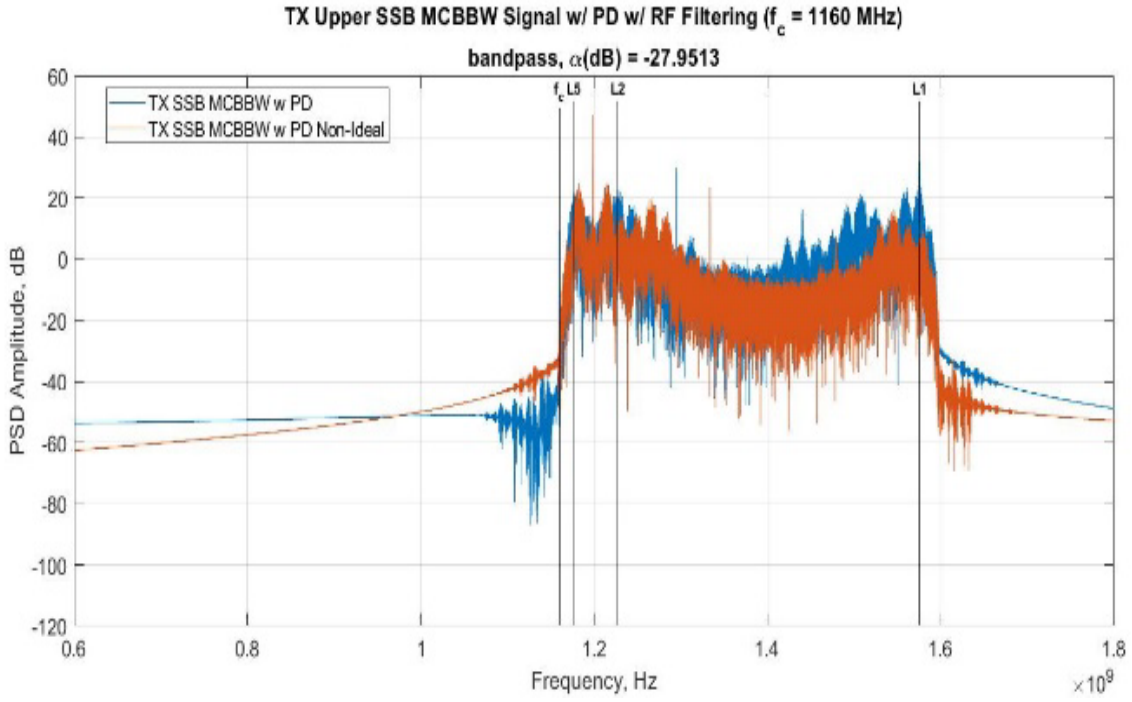

Figure 5.12: PSD of ideal and non-ideal MCBBW Signals with PD and with RF Filtering,

α(dB) = -27.95 dB, using the Bandpass Filter

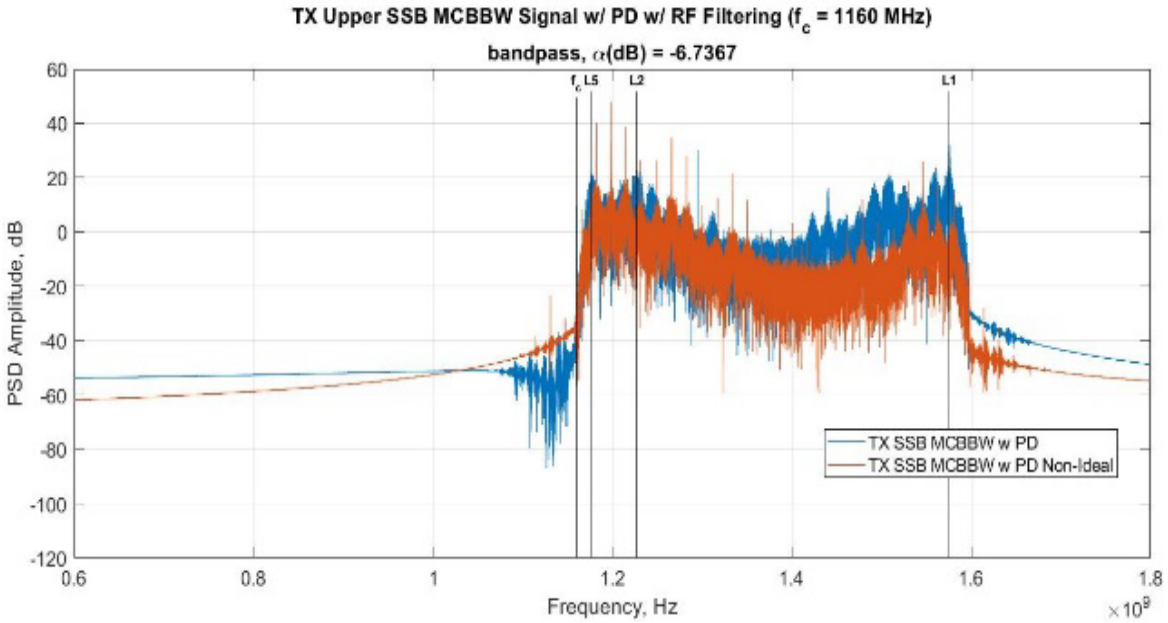

Figure 5.13: PSD of ideal and non-ideal MCBBW Signals with PD and with RF Filtering, α(dB) = -6.7367 dB, using Bandpass Filter

6. Conclusion and Way-Forward

With the development of ideal satellite system components' MATLAB models, our team has further implemented and simulated non-ideal system components into MATLAB, specifically the timing errors caused by the reference clock, the non-ideal subcarrier components and their parameters, the non-ideal phase modulation, non-ideal HPA model, and non-ideal RF filter with their own parameters. We set up the non-ideal MATLAB models using "in-spec" specifications and assess the effects of varied imbalanced amplitude (Γ) and imbalanced phase (θ) values on the proposed GNSS-MCBBW system performance. Various values of Γ and θ onto the signals were shown, changing the value of the undesired unsuppressed carrier signal component, α. We saw how Γ was the more influential parameter in determining the value of α in terms of dB. The PSDs of the varied subcarrier signals were plotted and compared for demonstration and analysis purposes. Significant degradation and spurious emissions exist among the entire signal, along with power loss on the L1 signal component. The PSD and modulation loss models were plotted for the GNSS SSB-MCBBW. The plots showed various stages of MCBBW signal, with either Hilbert transform or with BPF approach, with or without the HPA pre-distorter and RF filter, and through the HPA operating temperatures of 25°C, 27°C, and 30°C. This paper presented some key MATLAB simulation results associated with the non-ideal GNSS-MCBBW satellite system components. Additional results can be found in [5]. The non-ideal satellite system emulator has been used by our team to evaluate the signal classifier and operational environment predictor (OEP) using ML-AI [2].

Moving forward, our team has begun to optimize the emulator to find the modulation indices and other parameters that minimize our modulation losses within our signal. In addition, our team has completed a preliminary system performance assessment on the proposed (i) ML-AI HPA pre-distorter, (ii) operational environment predictor [2] and signal classifier using ML-AI [6], and (iii) GNSS-MACBBW receiver using HT [7] and BPF [8] signal processing. Moreover, any future work includes general GNSS applications and investigations to implement said system in the real world.

Correspondence
Dr. Tien M. Nguyen (CSUF POC), 800 N State College Blvd, Fullerton, CA 92831, e-mail: tmnguyen57@fullerton.edu.
Dr. Charles H. Lee, (CSUF Industrial Project for Graduate Program in Applied Mathematics, Director), 800 N State College Blvd, Fullerton, CA 92831, e-mail: charlesHLee@fullerton.edu.
Dr. Genshe Chen (Contract PM POC), 20271 Goldenrod Ln, Germantown, MD 20876, e-mail: gchen@intfusiontech.com.
Dr. Dan Shen (Contract Chief Engineer, Technical POC), 20271 Goldenrod Ln, Germantown, MD 20876, e-mail: dshen@intfusiontech.com.
Dr. Khanh D. Pham (AFRL PM POC), 3550 Aberdeen Avenue S.E., Kirtland AFB, NM 87117, e-mail: khanh.pham.1@ spaceforce.mil

Acknowledgment

The authors would like to thank Ms. Maria Rios, Technical Communication Specialist, IFT, for her support during the preparation of this paper.

References

[1] Tien M. Nguyen, Charles H. Lee, Yinwei Chen, Sam Behseta, Dan Shen, Genshe Chen, John Nguyen, Xiwen Kang, Khanh D. Pham, “Innovative Multicarrier Broadband Waveforms for Future GNSS Applications – A System Overview,” Accepted for presentation and publication in the 202 IEEE/ION Position Location and Navigation Symposium (PLANS) Proceedings, April 24 – 27, 2023, Monterey, California.

[2] Jose Mendez-Villanueva, Gustavo Sopena, Tien M. Nguyen, Charles H. Lee, Yinwei Chen, Sam Behseta, Dan Shen, Genshe Chen, John Nguyen, Xiwen Kang, Khanh D. Pham, "Innovative Multi-carrier Broadband Waveforms Classification Using Machine Learning for Future GNSS Applications,” Accepted for presentation and publication in the SPACEOPS 2023, The 17th International Conference on Space Operations, 6 – 10 March 2023, Dubai, United Arab Emirates.

[3] Tien M. Nguyen, “On the Effects of a Spacecraft Subcarrier Unbalanced Modulator, International Journal of Digital and Analog Communication Systems, Vol. 6, 183-192 (1993).

[4] Tien M. Nguyen; James Yoh; Charles H. Lee; Hien T. Tran; Diana M. Johnson, “Modeling of HPA and HPA linearization through a pre-distorter: Global Broadcasting Service applications,” IEEE Transactions on Broadcasting, Volume: 49, Issue: 2, June 2003.

[5] Charles Lee, Josselyn Romero, Leo Amador, Tien M. Nguyen, Genshe Chen, Dan Shen, Yinwei Chen, Non-Ideal GNSS-MCBBW Satellite System Modeling and Simulation, Final Report from IFT-CSUF Research Team as a requirement for the IPGPAM, May 2022.

[6] Tien M. Nguyen, Charles H. Lee, Jose Aguilar, Danny Paniagua-Rodriguez, Sam Behseta, Dan Shen, Genshe Chen, John Nguyen, Xiwen Kang, Khanh D. Pham, "HPA Pre-Distorter using Machine Learning and Artificial Intelligence for Future GNSS Applications," Accepted for presentation and publication in the 2023 SPIE Conference, 30 April-4 May 2023, Orlando, Florida.

[7] Tien M. Nguyen, Charles H. Lee, Sam Behseta, Dan Shen, Genshe Chen, John Nguyen, Xiwen Kang, Khanh D. Pham, "Hilbert Transform-MCBBW Ground Receiver Terminal for Future GNSS Applications," Accepted for presentation and publication in the 2023 IEEE/ION Position Location and Navigation Symposium (PLANS) Proceedings, April 24 – 27, 2023, Monterey, California.

[8] Aline Rohloff, Angelica Arredondo, Tien M. Nguyen, Charles H. Lee, Sam Behseta, Dan Shen, Genshe Chen, John Nguyen, Xiwen Kang, Khanh D. Pham, "BPF-MCBBW Ground Receiver Terminal for Future GNSS Applications," Accepted for presentation and publication in the 2023 IEEE/ION Position Location and Navigation Symposium (PLANS) Proceedings, April 24 – 27, 2023, Monterey, California.